Chemistry of a Light Impurity in a Bose-Einstein Condensate

Arthur Christianen,[1,2,*] J. Ignacio Cirac,[1,2] and Richard Schmidt[1,2,3,†]
[1]*Max-Planck-Institut für Quantenoptik, Hans-Kopfermann-Strasse 1, D-85748 Garching, Germany*
[2]*Munich Center for Quantum Science and Technology (MCQST), Schellingstraße 4, D-80799 Munich, Germany*
[3]*Department of Physics and Astronomy, Aarhus University, DK-8000 Aarhus C, Denmark*

(Received 27 October 2021; revised 30 March 2022; accepted 4 April 2022; published 4 May 2022)

Similar to an electron in a solid, an impurity in an atomic Bose-Einstein condensate (BEC) is dressed by excitations from the medium, forming a polaron quasiparticle with modified properties. This impurity can also undergo chemical recombination with atoms from the BEC, a process resonantly enhanced when universal three-body Efimov bound states cross the continuum. To study the interplay between these phenomena, we use a Gaussian state variational method able to describe both Efimov physics and arbitrarily many excitations of the BEC. We show that the polaron cloud contributes to bound state formation, leading to a shift of the Efimov resonance to smaller interaction strengths. This shifted scattering resonance marks the onset of a polaronic instability towards the decay into large Efimov clusters and fast recombination, offering a remarkable example of chemistry in a quantum medium.

DOI: 10.1103/PhysRevLett.128.183401

Studying chemical solvent effects on a fundamental level is challenging. The process of solvation plays an important role in chemistry, but typical solvents prohibit clean and controllable experiments or theoretical descriptions. Most experiments with the aim to understand collisions and reactions from first principles [1–14] are therefore carried out in gases, which are usually too dilute for medium effects to play a role.

Degenerate quantum gases [15–17], while not being solvents commonly found in chemical laboratories, offer a unique way to overcome these limitations. Here, the wave functions of the particles overlap even though the density is low. As a result, medium effects can be studied in a clean and controllable setting.

In this Letter, we consider an impurity atom immersed in an atomic Bose-Einstein condensate (BEC). In this scenario, the chemical medium effects are reminiscent of condensed matter physics. The impurity is namely dressed by excitations from the BEC to form a quasiparticle called Bose polaron [18–20], similar to the paradigmatic polarons found in solids [21–28]. At the same time, the impurity can undergo chemical reactions in the form of three-body recombination with BEC atoms [15]. This reaction forms one of the predominant loss mechanisms in BECs. The process involves two atoms decaying into a dimer state while a third atom takes away the released energy, leading to the expulsion of the reaction products from the trap.

In collisions and reactions at low temperatures, scattering resonances play a key role [29]. Such resonant enhancements of the scattering rate occur when the energy of a quasi-bound state matches the collision energy. Experiments probing scattering resonances [9–14] provide stringent tests for quantum chemistry methods [10] and their manipulation has important applications such as quantum simulation [30] or controlled chemistry [31,32]. In the case of three-body recombination, resonances are caused by a universal type of three-body bound states [33–39], that arise due to the Efimov effect [40,41].

The aim of our work is to describe how polaronic dressing of the impurities affects their Efimov scattering resonances and vice versa. The simultaneous description of both the correlations leading to the Efimov effect [42,43] and the formation of a macroscopic polaron cloud containing a large number of excitations [44,45], has so far remained an open challenge. We approach this problem using a variational method based on Gaussian states [46] in the impurity reference frame. We focus on the case of light impurities, where the Efimov effect is particularly prominent [36,37,41,47].

We find that the medium shifts the three-body scattering resonance to smaller interaction strengths because the polaron cloud assists bound state formation. Furthermore, we show that this shifted resonance marks the onset of a polaronic instability: when a bound state is formed this leads to a cascade into ever larger Efimov clusters, many-particle bound states forming due to the Efimov effect. Their existence has been theorized and demonstrated experimentally in the homonuclear case [41,48–50]. Here we predict that this extends to the heteronuclear case. In experiments the polaronic instability is heralded by rapid chemical recombination.

Model.—We consider an impurity of mass M immersed in a three dimensional, weakly interacting, homogeneous BEC of density n_0 at zero temperature, consisting of bosons of mass m. The interboson and impurity-boson scattering lengths are denoted by a_B and a, respectively, and correspond to coupling constants g_B and g. We use a single-channel Hamiltonian ($\hbar = 1$) with contact interactions, valid close to broad Feshbach resonances [9,51]:

$$\hat{\mathcal{H}}_0 = \int \frac{d^3k}{(2\pi)^3} \frac{\boldsymbol{k}^2}{2m} \hat{a}^\dagger_{\boldsymbol{k}} \hat{a}_{\boldsymbol{k}} + \frac{\hat{\boldsymbol{P}}^2}{2M} + g \int d^3r \delta(\boldsymbol{r} - \hat{\boldsymbol{R}}) \hat{a}^\dagger_{\boldsymbol{r}} \hat{a}_{\boldsymbol{r}} + \frac{g_B}{2} \int\int d^3r d^3r' \delta(\boldsymbol{r} - \boldsymbol{r}') \hat{a}^\dagger_{\boldsymbol{r}'} \hat{a}^\dagger_{\boldsymbol{r}} \hat{a}_{\boldsymbol{r}'} \hat{a}_{\boldsymbol{r}}. \quad (1)$$

The $\hat{a}^\dagger_{\boldsymbol{k}}$ are bosonic creation operators and the impurity is described with operators $\hat{\boldsymbol{P}}$ and $\hat{\boldsymbol{R}}$. After Bogoliubov transformation, introducing Bogoliubov quasiparticles with operators $\hat{b}^\dagger_{\boldsymbol{k}}$, $\hat{b}_{\boldsymbol{k}}$ and dispersion $\omega_k = \sqrt{(k^4/4m^2) + (g_B n_0 k^2/m)}$, we move to the reference frame of the impurity using the Lee-Low-Pines (LLP) transformation [52]. The total momentum of the system is set to zero, yielding the extended Fröhlich Hamiltonian [44,53]:

$$\hat{\mathcal{H}} = \int_{\boldsymbol{k}} \left(\omega_k + \frac{k^2}{2M}\right) \hat{b}^\dagger_{\boldsymbol{k}} \hat{b}_{\boldsymbol{k}} + \int_{\boldsymbol{k}} \int_{\boldsymbol{k}'} \frac{\boldsymbol{k} \cdot \boldsymbol{k}' \hat{b}^\dagger_{\boldsymbol{k}} \hat{b}^\dagger_{\boldsymbol{k}'} \hat{b}_{\boldsymbol{k}} \hat{b}_{\boldsymbol{k}'}}{2M} + g n_0 + g\sqrt{n_0} \int_{\boldsymbol{k}} W_k [\hat{b}^\dagger_{\boldsymbol{k}} + \hat{b}_{-\boldsymbol{k}}] + g \int_{\boldsymbol{k}} \int_{\boldsymbol{k}'} \left[V^{(1)}_{k,k'} \hat{b}^\dagger_{\boldsymbol{k}} \hat{b}_{\boldsymbol{k}'} + \frac{V^{(2)}_{k,k'}}{2} (\hat{b}^\dagger_{\boldsymbol{k}} \hat{b}^\dagger_{\boldsymbol{k}'} + \hat{b}_{-\boldsymbol{k}} \hat{b}_{-\boldsymbol{k}'}) \right], \quad (2)$$

where $W_k = (k/\sqrt{2m\omega_k})$ and $V^{(1,2)}_{k,k'} = (W_k W_{k'}/2) \pm [1/2(W_k W_{k'})]$. We use the notation $\int_{\boldsymbol{k}} \equiv \int_{|\boldsymbol{k}|<\Lambda} [d^3k/(2\pi)^3]$. Λ. A uv cutoff Λ is introduced to regularize the impurity-boson interaction and it serves as the three-body parameter. It is proportional to the inverse of the van der Waals length of the realistic scattering potential and can be fixed by matching the scattering length of the first Efimov resonance a_- to the experimentally observed value. We take the regularized contact interaction to only act on the s-wave components of the wave function.

We describe the bosonic excitations of the BEC by a variational Gaussian state ansatz [46]. This ansatz allows for an arbitrary number of excitations and pairwise interboson correlations. Importantly, by virtue of the LLP transformation also three-body correlations between two bosons and the impurity are fully included. The Gaussian state Ansatz can be written as

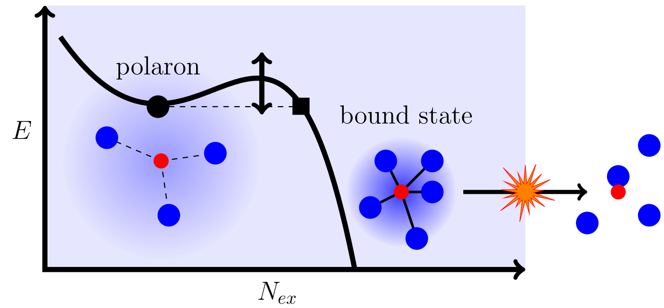

FIG. 1. Qualitative energy landscape. Illustration of the energy E of an impurity immersed in a BEC as a function of the number of excitations $N_{\rm ex}$ surrounding it. The local minimum corresponds to the polaron. It is separated by a barrier from states much lower in energy, represented by bound clusters containing a large number of particles. Experimentally, the formation of these clusters leads to fast recombination and loss. The barrier height is dependent on the density of the BEC and the scattering length. The barrier disappears at the density-dependent critical scattering length a^*, leading to a complete instability of the polaron. The black circle and square are discussed in the context of Fig. 4.

$$|\psi\rangle = \exp\left(\int_{\boldsymbol{k}} \hat{\Psi}^\dagger_{\boldsymbol{k}} \sigma^z \Phi_{\boldsymbol{k}}\right) \exp\left(\frac{i}{2} \int_{\boldsymbol{k}} \int_{\boldsymbol{k}'} \hat{\Psi}^\dagger_{\boldsymbol{k}} \Xi_{\boldsymbol{k},\boldsymbol{k}'} \hat{\Psi}_{\boldsymbol{k}'}\right) |\text{BEC}\rangle, \quad (3)$$

with Nambu vector $\hat{\Psi}_{\boldsymbol{k}} = (\hat{b}^\dagger_{\boldsymbol{k}}, \hat{b}_{\boldsymbol{k}})^T$, coherent displacement $\Phi_{\boldsymbol{k}} = \langle \hat{\Psi}_{\boldsymbol{k}} \rangle$, correlation matrix Ξ, and σ^z the Pauli z matrix. Both $\boldsymbol{\Phi}$ and Ξ are variational parameters which are optimized using imaginary time evolution [46]. Keeping only the coherent part of Eq. (3), one retrieves the mean field results from Ref. [44], that do not account for Efimov physics. We consider an exemplary mass ratio $M/m = 6/133$ of a ^{6}Li impurity in a ^{133}Cs BEC.

Qualitative picture.—Our key result is illustrated by Fig. 1, showing the energy landscape of the extended Fröhlich Hamiltonian at fixed background density and negative scattering length as a function of the number of excitations $N_{\rm ex} = \langle \int_{\boldsymbol{k}} \hat{b}^\dagger_{\boldsymbol{k}} \hat{b}_{\boldsymbol{k}} \rangle$ forming the dressing cloud of the impurity. At small excitation numbers we find a local minimum corresponding to the polaron, but for larger particle numbers there are lower energy states in the form of Efimov clusters. We predict that such Efimov clusters exist for a large range of interactions strengths and even in regimes where two- and three-body bound states are absent in the few-body problem ($|a| < |a_-|$). There is a barrier protecting the polaron from decaying into these clusters, whose height decreases as a function of interaction strength. At a density-dependent critical scattering length a^* the barrier completely disappears and the polaron breaks down. Below we show that the onset of this polaronic instability represents a many-body shifted Efimov scattering resonance. Beyond the instability, polarons quickly decay into Efimov clusters. Because these clusters contain many particles in close proximity, they in turn rapidly disintegrate due to recombination.

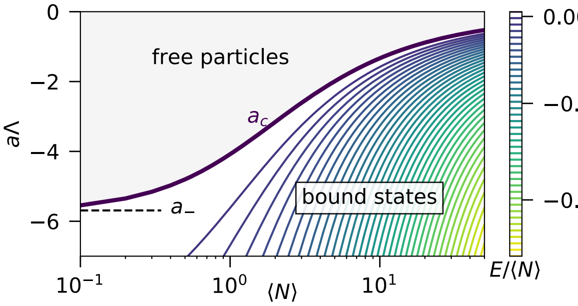

FIG. 2. Efimov cluster formation. Contour plot of the binding energy per particle $E/\langle\hat{N}\rangle$ (in units of Λ^2/M) as a function of the expectation value of the number of particles $\langle\hat{N}\rangle$ and scattering length a, for mass ratio $M/m = 6/133$. The bold line indicates the critical scattering length a_c at which a bound state first appears. The noninteger particle numbers follow from our variational wave function being a superposition of different particle number eigenstates.

Formation of Efimov clusters.—First we demonstrate the existence of the deeply-bound, many-body Efimov clusters illustrated in the right part of Fig. 1. For identical bosons a simple dimensional argument suffices to show that Efimov clusters containing more and more particles get ever more strongly bound: the binding energy scales with N^2 while the counteracting kinetic energy only scales with N [41]. In our heteronuclear case, where the bosons interact with the impurity but not with each other, the situation is not as obvious since now also the binding energy scales with N.

We now demonstrate that the same trend as in the homonuclear case persists in our model for noninteracting bosons ($a_B = 0$); i.e., we show that the binding energy keeps increasing as the number of particles in the bound state increases. To tackle this problem, instead of exactly solving the N-body problem for which the complexity grows exponentially with N, we employ a variational Gaussian state (without its coherent part) which greatly reduces computational complexity.

Gaussian states consist of a superposition of states of even boson number, and we thus derive a variational bound on the energy for fixed *average* particle number $\langle\hat{N}\rangle$. The minimization is performed using imaginary time evolution [46] including a dynamically changing chemical potential to keep $\langle\hat{N}\rangle$ constant [54].

In Fig. 2 we show a contour plot of the energy per particle $E/\langle\hat{N}\rangle$ as a function of $\langle\hat{N}\rangle$ and a, at $n_0 = 0$. We find that $|E|/\langle\hat{N}\rangle$ increases monotonically with $\langle\hat{N}\rangle$ and $|a|$. The purple solid line shows the critical scattering length a_c at which bound state formation, signaled by $E/\langle\hat{N}\rangle < 0$, sets in. Beyond this point *all* particles in the system are bound to the impurity. For small $\langle\hat{N}\rangle \ll 1$, a_c approaches the three-body result $a_- \approx -5.7\Lambda^{-1}$. In this regime, the Gaussian State can be approximated by

$$|\psi\rangle \approx \left(1 + \frac{i}{2}\hat{\mathbf{\Psi}}^\dagger \Xi \hat{\mathbf{\Psi}}\right)|0\rangle, \tag{4}$$

and the energy of the state is thus entirely determined by the $N = 2$ component of the wave function. Hence, the Efimov scattering length a_- is recovered. For increasing $\langle\hat{N}\rangle$, $|a_c|$ decreases and slowly converges to a small but nonzero value determined by zero-point motion [55].

Altogether we see that the more particles the cluster contains, the more strongly it becomes bound. Similarly, the more particles in the cluster, the smaller the scattering length required for its formation. This "cooperative binding" effect is caused by impurity-mediated interactions between the bosons, governed by the second term in Eq. (2). Since this term originates from the LLP transformation acting on the impurity momentum operator [44,55], the driving force of the cluster formation can be understood as arising from an increasingly efficient use of the kinetic energy of the impurity.

Since the binding energy per particle increases monotonically with $\langle\hat{N}\rangle$, also the total energy grows without bound. Therefore, the ground state of the Hamiltonian is a bound state containing all particles in the system. Because such states are tightly bound on scales much smaller than the typical interparticle distance in the BEC, the effect of the medium on their energy is relatively small [55]. Including interboson repulsion will limit both the energy and the number of bound particles, and modify the spatial structure of the clusters. However, as long as the repulsion is small, these effects are negligible for a description of typical cold atom experiments, where recombination reactions will occur long before a large particle number has a chance to build up. Note that on a Bogoliubov level the inclusion of a interboson repulsion only modifies the long-wavelength behavior of the bosons and thus barely affects the tightly bound states.

Metastable polaron.—We have now established that the ground state of the extended Fröhlich Hamiltonian is not a polaronic, but a many-body bound state. However, to dynamically form such a many-body bound state from a homogeneous BEC, all participating atoms need to simultaneously come together into a small volume. Since this is an extremely unlikely process, it can be expected that the polaron remains a metastable excited state of the Hamiltonian.

To corroborate this picture quantitatively, we start by finding a local energy minimum on the variational manifold at small $a < 0$ and constant background density. This is simple, since this local minimum is close to the mean field solution and even captured by the original Fröhlich model. The wave function and energy of the local minimum are then updated for increasing $|a|$. Crucially, we find that as a critical scattering length a^* is reached, the minimum turns into a saddle point, leading to a divergence of the particle number and energy: the polaron has become unstable.

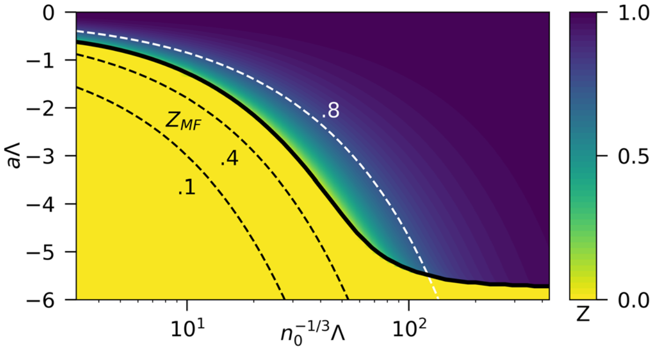

FIG. 3. Polaron instability and shifted Efimov scattering resonance. The critical scattering length a^* at which the polaron breaks down (black solid) as a function of the mean interparticle distance $n_0^{-1/3}\Lambda$, for $M/m = 6/133$ and $a_B\Lambda = 0.1$. The color map shows the quasiparticle weight Z. Dashed lines indicate Z_{MF} from mean field theory.

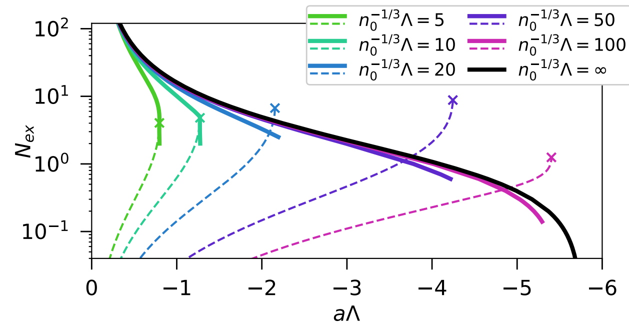

FIG. 4. Mechanism of the resonance shift. The number of excitations in the polaron cloud N_{ex} (dashed lines) as a function of scattering length $a\Lambda$ at various densities n_0 (indicated by color). The number of excitations needed to form a bound state with lower energy than the polaron energy is shown using solid lines. Crosses indicate the points at which the polaron destabilizes. Parameters as in Fig. 3.

In Fig. 3 we plot a^* as a function of the average interbosonic distance $n_0^{-1/3}\Lambda$ as a solid black line. We have used an interboson scattering length $a_B = 0.1\ \Lambda^{-1}$ that keeps the size of the polaron cloud finite [45], but which is small enough for the Bogoliubov approximation to remain valid. In the background of Fig. 3, the quasiparticle weight $Z = |\langle\psi|\mathrm{BEC}\rangle|^2$ is shown as a color map. The dashed lines show contours of Z obtained from mean-field theory. While the polaron energy only experiences a small shift ($< 10\%$) compared to the mean field result [55], the quasiparticle weight is drastically affected by introducing interboson correlations, especially close to the instability, where Z drops to zero.

Polaron instability and shifted Efimov resonance.—We now consider further the origin of the instability at a^*, corresponding to the black solid line in Fig. 3. In contrast to the vacuum case, the background medium can take away energy and add particles. Together with the cooperative binding effect this means that as soon as a bound state can be formed, this will cause a cascade into ever larger Efimov clusters, and hence an instability.

The onset of the instability found using Gaussian states can be interpreted as a shifted Efimov resonance. The instability, namely, occurs when the polaron is no longer stable against the included perturbations, which are single and double excitations on top of the BEC. In other words, the instability happens when a bound state can be formed between the polaron and one or two additional particles, immediately showing the connection to the Efimov scattering resonance. As a confirmation, we see that a^* reduces to a_- in the low density limit.

We can thus conclude that Fig. 3 is a quantitative prediction of the medium-induced shift of the Efimov scattering resonance. In terms of the scattering length, this shift is more than a factor 2, demonstrating that a quantum mechanical solvent can strongly affect ultracold chemistry.

Interestingly, the behavior of the resonance turning into an instability is qualitatively different from the predictions in Refs. [42,43,56]. There, a smooth crossover from a polaron into an Efimov state is predicted in the case of an equal mass impurity in a BEC. This shows that the effects of a quantum medium can be quite diverse, depending on the character of the solvent, the solute, and their interactions.

The origin of the resonance shift in our model can be explained with the help of Fig. 4. Here we consider the number of excitations N_{ex} in the polaron cloud (dashed lines, corresponding to the black dot in Fig. 1) and the number of excitations needed to form a many-body bound state lower in energy than the polaron (solid lines, black square in Fig. 1) as a function a for several values of n_0. The crosses at the end of the dashed lines indicate the points given by a^*. The black solid line corresponds to the scattering length a_c in Fig. 2.

Following the dashed lines, we see that the number of excitations in the polaron cloud increases as a function of $|a|$. For small $|a|$, N_{ex} is too small to facilitate cluster formation and the polaron thus remains metastable. When N_{ex}, however, matches or exceeds the number of particles needed to form a bound state, the polaron becomes unstable.

The larger the BEC density, the more excitations the polaron cloud contains at a given a (upward shift of the dashed lines) and the sooner the instability occurs. A smaller contribution to this effect is a shift of the colored solid lines with respect to the black line, which indicate a stabilization of the Efimov clusters due to the linear Fröhlich term. This explains the underlying physical mechanism of the shift of the Efimov scattering resonance to smaller interaction strengths as a function of background density.

Surprisingly, for low densities there is a small regime in Fig. 4 where the polaron remains metastable even though it contains enough particles to lead to an instability. Here the extent of the polaron cloud is much larger than the size of Efimov clusters, so that the bosons furthest from the impurity do not participate in the cluster formation [55].

Experimental implementation.—To observe our findings, one may consider using light impurities such as Li in a BEC of K [57], Rb [38] or Cs atoms [36,37,58], where the Efimov effect is most prominent. Naturally, our results can be observed in three-body loss measurements, extending the observation of the Efimov effect [36,37] from a dilute thermal cloud to a high density BEC. After adiabatic preparation of the polaron state by a ramp of the magnetic field, crossing the instability of the polaron should lead to a drastic enhancement of atom loss through recombination reactions. This loss enhancement can then be measured as a function of the density. The loss measurement could be complemented by injection spectroscopy [18–20] since the strong decrease in quasiparticle weight close to the polaron instability should be accompanied by a significant broadening of the polaron spectral line. In injection spectroscopy also excited Efimov states, beyond the scope of the present work, could be observed when favorable mass ratios are used [47].

Conclusion.—Using a variational method based on Gaussian states, we have explored an example of chemistry in a quantum solvent by studying the heteronuclear Efimov scattering resonance of an impurity in a BEC. We have shown how Efimov resonances are shifted to smaller interaction strengths due to polaronic dressing of an impurity and a cooperative binding effect. Furthermore, in the medium the Efimov resonance turns into the onset of a polaronic instability towards Efimov cluster formation causing subsequent chemical recombination. Our findings can be probed using three-body loss measurements supported by radiofrequency spectroscopy.

Access to the real-time evolution would allow the computation of spectral functions, thus addressing physics beyond the instability. However, the study of the real-time dynamics of the polaron [59] with Gaussian states remains a challenge. Furthermore, studying the quantum dynamics is key to answering open questions about the competition between few-body recombination and formation of many-body correlated states. Related venues include competition between Auger recombination of excitons in semiconductors and formation of strongly correlated exciton liquids [60,61]. Our results may enable further studies of the bipolaron problem [62–64] where medium-induced polaron-polaron interactions become crucial, and provide new insight into the role three-body correlations play in many-body systems such as quenched BECs [55,65–73].

The authors thank T. Guaita and T. Shi for useful discussions. J. I. C. acknowledges funding from ERC Advanced Grant QENOCOBA under the EU Horizon 2020 program (Grant Agreement No. 742102). The authors acknowledge support from the Deutsche Forschungsgemeinschaft (DFG, German Research Foundation) under Germany's Excellence Strategy-EXC-2111-390814868.

*arthur.christianen@mpq.mpg.de
†richard.schmidt@mpq.mpg.de

[1] H. Pan, F. Wang, G. Czakó, and K. Liu, Direct mapping of the angle-dependent barrier to reaction for Cl + CHD 3 using polarized scattering data, Nat. Chem. **9**, 1175 (2017).

[2] Z. Gao, T. Karman, S. N. Vogels, M. Besemer, A. van der Avoird, G. C. Groenenboom, and S. Y. van de Meerakker, Observation of correlated excitations in bimolecular collisions, Nat. Chem. **10**, 469 (2018).

[3] D. Yuan, Y. Guan, W. Chen, H. Zhao, S. Yu, C. Luo, Y. Tan, T. Xie, X. Wang, Z. Sun *et al.*, Observation of the geometric phase effect in the H+ HD H2+ D reaction, Science **362**, 1289 (2018).

[4] S. D. Gordon, J. J. Omiste, J. Zou, S. Tanteri, P. Brumer, and A. Osterwalder, Quantum-state-controlled channel branching in cold Ne (3P2)+ Ar chemi-ionization, Nat. Chem. **10**, 1190 (2018).

[5] A. Kilaj, H. Gao, D. Rösch, U. Rivero, J. Küpper, and S. Willitsch, Observation of different reactivities of para and ortho-water towards trapped diazenylium ions, Nat. Commun. **9**, 2096 (2018).

[6] M.-G. Hu, Y. Liu, D. D. Grimes, Y.-W. Lin, A. H. Gheorghe, R. Vexiau, N. Bouloufa-Maafa, O. Dulieu, T. Rosenband, and K.-K. Ni, Direct observation of bimolecular reactions of ultracold KRb molecules, Science **366**, 1111 (2019).

[7] Y. Liu, M.-G. Hu, M. A. Nichols, D. D. Grimes, T. Karman, H. Guo, and K.-K. Ni, Photo-excitation of long-lived transient intermediates in ultracold reactions, Nat. Phys. **16**, 1132 (2020).

[8] M.-G. Hu, Y. Liu, M. A. Nichols, L. Zhu, G. Quéméner, O. Dulieu, and K.-K. Ni, Nuclear spin conservation enables state-to-state control of ultracold molecular reactions, Nat. Chem. **13**, 435 (2021).

[9] C. Chin, R. Grimm, P. Julienne, and E. Tiesinga, Feshbach resonances in ultracold gases, Rev. Mod. Phys. **82**, 1225 (2010).

[10] S. N. Vogels, T. Karman, J. Kłos, M. Besemer, J. Onvlee, A. van der Avoird, G. C. Groenenboom, and S. Y. van de Meerakker, Scattering resonances in bimolecular collisions between NO radicals and H 2 challenge the theoretical gold standard, Nat. Chem. **10**, 435 (2018).

[11] H. Yang, D.-C. Zhang, L. Liu, Y.-X. Liu, J. Nan, B. Zhao, and J.-W. Pan, Observation of magnetically tunable Feshbach resonances in ultracold 23Na40 K+ 40 K collisions, Science **363**, 261 (2019).

[12] T. de Jongh, M. Besemer, Q. Shuai, T. Karman, A. van der Avoird, G. C. Groenenboom, and S. Y. van de Meerakker, Imaging the onset of the resonance regime in low-energy NO-He collisions, Science **368**, 626 (2020).

[13] P. Paliwal, N. Deb, D. M. Reich, A. van der Avoird, C. P. Koch, and E. Narevicius, Determining the nature of quantum resonances by probing elastic and reactive scattering in cold collisions, Nat. Chem. **13**, 94 (2021).

[14] T. de Jongh, Q. Shuai, G. L. Abma, S. Kuijpers, M. Besemer, A. van der Avoird, G. C. Groenenboom, and

S. Y. van de Meerakker, Mapping partial wave dynamics in scattering resonances by rotational de-excitation collisions, Nat. Chem. 1 (2022).10.1038/s41557-022-00896-2.

[15] C. J. Pethick and H. Smith, *Bose-Einstein Condensation in Dilute Gases* (Cambridge University Press, Cambridge, England, 2008).

[16] S. Giorgini, L. P. Pitaevskii, and S. Stringari, Theory of ultracold atomic Fermi gases, Rev. Mod. Phys. **80**, 1215 (2008).

[17] L. De Marco, G. Valtolina, K. Matsuda, W. G. Tobias, J. P. Covey, and J. Ye, A degenerate Fermi gas of polar molecules, Science **363**, 853 (2019).

[18] N. B. Jørgensen, L. Wacker, K. T. Skalmstang, M. M. Parish, J. Levinsen, R. S. Christensen, G. M. Bruun, and J. J. Arlt, Observation of Attractive and Repulsive Polarons in a Bose-Einstein Condensate, Phys. Rev. Lett. **117**, 055302 (2016).

[19] M.-G. Hu, M. J. Van de Graaff, D. Kedar, J. P. Corson, E. A. Cornell, and D. S. Jin, Bose Polarons in the Strongly Interacting Regime, Phys. Rev. Lett. **117**, 055301 (2016).

[20] Z. Z. Yan, Y. Ni, C. Robens, and M. W. Zwierlein, Bose polarons near quantum criticality, Science **368**, 190 (2020).

[21] L. Landau, Über die Bewegung der Elektronen in Kristallgitter, Phys. Z. Sowjetunion **3**, 644 (1933).

[22] A. S. Alexandrov and J. T. Devreese, *Advances in Polaron Physics* (Springer, New York, 2010), Vol. 159.

[23] H. Zhu, K. Miyata, Y. Fu, J. Wang, P. P. Joshi, D. Niesner, K. W. Williams, S. Jin, and X.-Y. Zhu, Screening in crystalline liquids protects energetic carriers in hybrid perovskites, Science **353**, 1409 (2016).

[24] K. Miyata, D. Meggiolaro, M. T. Trinh, P. P. Joshi, E. Mosconi, S. C. Jones, F. De Angelis, and X.-Y. Zhu, Large polarons in lead halide perovskites, Sci. Adv. **3**, e1701217 (2017).

[25] J. E. Katz, X. Zhang, K. Attenkofer, K. W. Chapman, C. Frandsen, P. Zarzycki, K. M. Rosso, R. W. Falcone, G. A. Waychunas, and B. Gilbert, Electron small polarons and their mobility in iron (oxyhydr)oxide nanoparticles, Science **337**, 1200 (2012).

[26] C. Verdi, F. Caruso, and F. Giustino, Origin of the crossover from polarons to Fermi liquids in transition metal oxides, Nat. Commun. **8**, 15769 (2017).

[27] E. K. Salje, A. Alexandrov, and W. Liang, *Polarons and Bipolarons in High-T_c Superconductors and Related Materials* (Cambridge University Press, Cambridge, England, 2005).

[28] S. Zhang, T. Wei, J. Guan, Q. Zhu, W. Qin, W. Wang, J. Zhang, E. W. Plummer, X. Zhu, Z. Zhang, and J. Guo, Enhanced Superconducting State in FeSe/srtio_3 by a Dynamic Interfacial Polaron Mechanism, Phys. Rev. Lett. **122**, 066802 (2019).

[29] *Cold Chemistry*, edited by O. Dulieu and A. Osterwalder, Theoretical and Computational Chemistry Series (The Royal Society of Chemistry, 2018), pp. P001–670.

[30] I. Bloch, J. Dalibard, and S. Nascimbene, Quantum simulations with ultracold quantum gases, Nat. Phys. **8**, 267 (2012).

[31] R. V. Krems, Cold controlled chemistry, Phys. Chem. Chem. Phys. **10**, 4079 (2008).

[32] J.-R. Li, W. G. Tobias, K. Matsuda, C. Miller, G. Valtolina, L. De Marco, R. R. Wang, L. Lassablière, G. Quéméner, J. L. Bohn, and J. Ye, Tuning of dipolar interactions and evaporative cooling in a three-dimensional molecular quantum gas, Nat. Phys. **17**, 1144 (2021).

[33] T. Kraemer, M. Mark, P. Waldburger, J. G. Danzl, C. Chin, B. Engeser, A. D. Lange, K. Pilch, A. Jaakkola, H.-C. Nägerl, and R. Grimm, Evidence for Efimov quantum states in an ultracold gas of caesium atoms, Nature (London) **440**, 315 (2006).

[34] S. E. Pollack, D. Dries, and R. G. Hulet, Universality in three-and four-body bound states of ultracold atoms, Science **326**, 1683 (2009).

[35] M. Zaccanti, B. Deissler, C. D'Errico, M. Fattori, M. Jona-Lasinio, S. Müller, G. Roati, M. Inguscio, and G. Modugno, Observation of an Efimov spectrum in an atomic system, Nat. Phys. **5**, 586 (2009).

[36] R. Pires, J. Ulmanis, S. Häfner, M. Repp, A. Arias, E. D. Kuhnle, and M. Weidemüller, Observation of Efimov Resonances in a Mixture with Extreme Mass Imbalance, Phys. Rev. Lett. **112**, 250404 (2014).

[37] S.-K. Tung, K. Jiménez-García, J. Johansen, C. V. Parker, and C. Chin, Geometric Scaling of Efimov States in a $^6\mathrm{Li}-{}^{133}\mathrm{Cs}$ Mixture, Phys. Rev. Lett. **113**, 240402 (2014).

[38] R. A. W. Maier, M. Eisele, E. Tiemann, and C. Zimmermann, Efimov Resonance and Three-Body Parameter in a Lithium-Rubidium Mixture, Phys. Rev. Lett. **115**, 043201 (2015).

[39] J. Johansen, B. DeSalvo, K. Patel, and C. Chin, Testing universality of Efimov physics across broad and narrow Feshbach resonances, Nat. Phys. **13**, 731 (2017).

[40] V. Efimov, Energy levels arising from resonant two-body forces in a three-body system, Phys. Lett. B **33**, 563 (1970).

[41] P. Naidon and S. Endo, Efimov physics: A review, Rep. Prog. Phys. **80**, 056001 (2017).

[42] J. Levinsen, M. M. Parish, and G. M. Bruun, Impurity in a Bose-Einstein Condensate and the Efimov Effect, Phys. Rev. Lett. **115**, 125302 (2015).

[43] S. M. Yoshida, S. Endo, J. Levinsen, and M. M. Parish, Universality of an Impurity in a Bose-Einstein Condensate, Phys. Rev. X **8**, 011024 (2018).

[44] Y. E. Shchadilova, R. Schmidt, F. Grusdt, and E. Demler, Quantum Dynamics of Ultracold Bose Polarons, Phys. Rev. Lett. **117**, 113002 (2016).

[45] N.-E. Guenther, R. Schmidt, G. M. Bruun, V. Gurarie, and P. Massignan, Mobile impurity in a Bose-Einstein condensate and the orthogonality catastrophe, Phys. Rev. A **103**, 013317 (2021).

[46] T. Shi, E. Demler, and J. Ignacio Cirac, Variational study of fermionic and bosonic systems with non-Gaussian states: Theory and applications, Ann. Phys. (Amsterdam) **390**, 245 (2018).

[47] M. Sun and X. Cui, Enhancing the Efimov correlation in Bose polarons with large mass imbalance, Phys. Rev. A **96**, 022707 (2017).

[48] F. Ferlaino, S. Knoop, M. Berninger, W. Harm, J. P. D'Incao, H.-C. Nägerl, and R. Grimm, Evidence for Universal Four-Body States Tied to an Efimov Trimer, Phys. Rev. Lett. **102**, 140401 (2009).

[49] J. von Stecher, Five- and Six-Body Resonances Tied to an Efimov Trimer, Phys. Rev. Lett. **107**, 200402 (2011).

[50] A. Zenesini, B. Huang, M. Berninger, S. Besler, H.-C. Nägerl, F. Ferlaino, R. Grimm, C. H. Greene, and J. von Stecher, Resonant five-body recombination in an ultracold gas of bosonic atoms, New J. Phys. **15**, 043040 (2013).
[51] I. Bloch, J. Dalibard, and W. Zwerger, Many-body physics with ultracold gases, Rev. Mod. Phys. **80**, 885 (2008).
[52] T. D. Lee, F. E. Low, and D. Pines, The motion of slow electrons in a polar crystal, Phys. Rev. **90**, 297 (1953).
[53] S. P. Rath and R. Schmidt, Field-theoretical study of the Bose polaron, Phys. Rev. A **88**, 053632 (2013).
[54] T. Shi, E. Demler, and J. I. Cirac, Variational Approach for Many-Body Systems at Finite Temperature, Phys. Rev. Lett. **125**, 180602 (2020).
[55] A. Christianen, J. I. Cirac, and R. Schmidt, companion paper, Bose polaron and the Efimov effect: A Gaussian-state approach, Phys. Rev. A **105**, 053302 (2022).
[56] L. A. Peña Ardila and S. Giorgini, Impurity in a Bose-Einstein condensate: Study of the attractive and repulsive branch using quantum Monte Carlo methods, Phys. Rev. A **92**, 033612 (2015).
[57] B. Huang, I. Fritsche, R. S. Lous, C. Baroni, J. T. M. Walraven, E. Kirilov, and R. Grimm, Breathing mode of a Bose-Einstein condensate repulsively interacting with a fermionic reservoir, Phys. Rev. A **99**, 041602(R) (2019).
[58] B. J. DeSalvo, K. Patel, G. Cai, and C. Chin, Observation of fermion-mediated interactions between bosonic atoms, Nature (London) **568**, 61 (2019).
[59] M. Drescher, M. Salmhofer, and T. Enss, Real-space dynamics of attractive and repulsive polarons in Bose-Einstein condensates, Phys. Rev. A **99**, 023601 (2019).
[60] G. Wang, A. Chernikov, M. M. Glazov, T. F. Heinz, X. Marie, T. Amand, and B. Urbaszek, Colloquium: Excitons in atomically thin transition metal dichalcogenides, Rev. Mod. Phys. **90**, 021001 (2018).
[61] T. Mueller and E. Malic, Exciton physics and device application of two-dimensional transition metal dichalcogenide semiconductors, 2D Mater. Appl. **2**, 1 (2018).
[62] A. Camacho-Guardian, L. A. Peña Ardila, T. Pohl, and G. M. Bruun, Bipolarons in a Bose-Einstein Condensate, Phys. Rev. Lett. **121**, 013401 (2018).
[63] P. Naidon, Two impurities in a Bose-Einstein condensate: From Yukawa to Efimov attracted polarons, J. Phys. Soc. Jpn. **87**, 043002 (2018).
[64] G. Panochko and V. Pastukhov, Two- and three-body effective potentials between impurities in ideal BEC, J. Phys. A **54**, 085001 (2021).
[65] P. Makotyn, C. E. Klauss, D. L. Goldberger, E. A. Cornell, and D. S. Jin, Universal dynamics of a degenerate unitary Bose gas, Nat. Phys. **10**, 116 (2014).
[66] S. Piatecki and W. Krauth, Efimov-driven phase transitions of the unitary Bose gas, Nat. Commun. **5**, 3503 (2014).
[67] U. Eismann, L. Khaykovich, S. Laurent, I. Ferrier-Barbut, B. S. Rem, A. T. Grier, M. Delehaye, F. Chevy, C. Salomon, L.-C. Ha, and C. Chin, Universal Loss Dynamics in a Unitary Bose Gas, Phys. Rev. X **6**, 021025 (2016).
[68] C. E. Klauss, X. Xie, C. Lopez-Abadia, J. P. D'Incao, Z. Hadzibabic, D. S. Jin, and E. A. Cornell, Observation of Efimov Molecules Created from a Resonantly Interacting Bose Gas, Phys. Rev. Lett. **119**, 143401 (2017).
[69] V. E. Colussi, J. P. Corson, and J. P. D'Incao, Dynamics of Three-Body Correlations in Quenched Unitary Bose Gases, Phys. Rev. Lett. **120**, 100401 (2018).
[70] C. Eigen, J. A. Glidden, R. Lopes, E. A. Cornell, R. P. Smith, and Z. Hadzibabic, Universal prethermal dynamics of Bose gases quenched to unitarity, Nature (London) **563**, 221 (2018).
[71] J. P. D'Incao, J. Wang, and V. E. Colussi, Efimov Physics in Quenched Unitary Bose Gases, Phys. Rev. Lett. **121**, 023401 (2018).
[72] V. E. Colussi, H. Kurkjian, M. Van Regemortel, S. Musolino, J. van de Kraats, M. Wouters, and S. J. J. M. F. Kokkelmans, Cumulant theory of the unitary Bose gas: Prethermal and Efimovian dynamics, Phys. Rev. A **102**, 063314 (2020).
[73] S. Musolino, H. Kurkjian, M. V. Regemortel, M. Wouters, S. J. J. M. F. Kokkelmans, and V. E. Colussi, Bose-Einstein Condensation of Efimovian Triples in the Unitary Bose Gas, Phys. Rev. Lett. **128**, 020401 (2022).